PECTIN METHYLESTERASE48 Is Involved in Arabidopsis Pollen Grain Germination[1][OPEN]

Christelle Leroux, Sophie Bouton, Marie-Christine Kiefer-Meyer, Tohnyui Ndinyanka Fabrice, Alain Mareck, Stéphanie Guénin, Françoise Fournet, Christoph Ringli, Jérôme Pelloux, Azeddine Driouich, Patrice Lerouge, Arnaud Lehner[2], and Jean-Claude Mollet[2]*

Laboratoire Glycobiologie et Matrice Extracellulaire, Normandie Université, Institute for Research and Innovation in Biomedicine, Végétal, Agronomie, Sol, et Innovation, 76821 Mont-Saint-Aignan, France (C.L., M.-C.K.-M., A.M., A.D., P.L., A.L., J.-C.M.); Unité Biologie des Plantes et Innovation (S.B., S.G., F.F., J.P.) and Centre de Ressources Régionales en Biologie Moléculaire (S.G.), Université de Picardie Jules Verne, 80039 Amiens, France; and Institute of Plant Biology, University of Zürich, 8008 Zurich, Switzerland (T.N.F., C.R.)

Germination of pollen grains is a crucial step in plant reproduction. However, the molecular mechanisms involved remain unclear. We investigated the role of PECTIN METHYLESTERASE48 (PME48), an enzyme implicated in the remodeling of pectins in Arabidopsis (*Arabidopsis thaliana*) pollen. A combination of functional genomics, gene expression, in vivo and in vitro pollen germination, immunolabeling, and biochemical analyses was used on wild-type and *Atpme48* mutant plants. We showed that *AtPME48* is specifically expressed in the male gametophyte and is the second most expressed *PME* in dry and imbibed pollen grains. Pollen grains from homozygous mutant lines displayed a significant delay in imbibition and germination in vitro and in vivo. Moreover, numerous pollen grains showed two tips emerging instead of one in the wild type. Immunolabeling and Fourier transform infrared analyses showed that the degree of methylesterification of the homogalacturonan was higher in *pme48−/−* pollen grains. In contrast, the PME activity was lower in *pme48−/−*, partly due to a reduction of PME48 activity revealed by zymogram. Interestingly, the wild-type phenotype was restored in *pme48−/−* with the optimum germination medium supplemented with 2.5 mM calcium chloride, suggesting that in the wild-type pollen, the weakly methylesterified homogalacturonan is a source of Ca^{2+} necessary for pollen germination. Although pollen-specific PMEs are traditionally associated with pollen tube elongation, this study provides strong evidence that PME48 impacts the mechanical properties of the intine wall during maturation of the pollen grain, which, in turn, influences pollen grain germination.

Sexual plant reproduction requires the growth of tip-polarized pollen tubes through the female tissues in order to deliver the two sperm cells to the embryo sac. Despite the importance of this crucial step that leads to seed production, the molecular mechanisms implicated in the spatial and temporal controls of pollen tube growth are not fully known (Johnson and Lord, 2006; Palanivelu and Tsukamoto, 2012). However, it has been proposed that the modulation of the stiffness of the pollen tube was important during pollen tube growth (Parre and Geitmann, 2005a; Fayant et al., 2010; Vogler et al., 2013). Pollen tube elongation is highly polarized, with the growth area being restricted to the apex of the tube. New membranes and cell wall materials are rapidly secreted at the tip, providing the building material necessary to sustain the fast pollen tube growth (Bove et al., 2008; Guan et al., 2013). The pollen tube cell wall of many species, including tobacco (*Nicotiana tabacum*; Li et al., 1995; Ferguson et al., 1998), lily (*Lilium longiflorum*; Roy et al., 1997), and Arabidopsis (*Arabidopsis thaliana*; Lennon and Lord, 2000; Dardelle et al., 2010), is characterized by one layer in the tip region and two distinguishable layers back in the shank. Back from the tip, the inner layer is mainly composed of callose, a (1,3)-β-glucan, which is not detectable in the tip region in normal growth conditions (Ferguson et al., 1998; Derksen et al., 2002; Parre and Geitmann, 2005b; Dardelle et al., 2010; Chebli et al., 2012). Moreover, callose is also deposited periodically within the pollen tube to form plugs that maintain the tube cell in the expanding apical region. The outer cell wall in the tip and back from the tip is mostly composed of pectins, xyloglucan, cellulose, and proteoglycans such as arabinogalactan proteins (Geitmann and Steer, 2006; Dardelle et al., 2010; Chebli et al., 2012; Nguema-Ona et al., 2012).

In eudicot species, pectins constitute a major portion of the primary cell wall. Pectins are complex polysaccharides consisting of homogalacturonan (HG), rhamnogalacturonan I,

[1] This work was supported by the Institute for Research and Innovation in Biomedicine of the region Haute-Normandie, France (to C.L.), by the University of Rouen, and by the Trans Channel Wallnet project that was selected by the INTERREG IVA program, France (Channel)-England European cross-border cooperation program, financed by the European Regional Development Fund.

[2] These authors contributed equally to the article.

* Address correspondence to jean-claude.mollet@univ-rouen.fr.

The author responsible for distribution of materials integral to the findings presented in this article in accordance with the policy described in the Instructions for Authors (www.plantphysiol.org) is: Jean-Claude Mollet (jean-claude.mollet@univ-rouen.fr).

[OPEN] Articles can be viewed without a subscription.

www.plantphysiol.org/cgi/doi/10.1104/pp.114.250928

rhamnogalacturonan II, and xylogalacturonan (Vincken et al., 2003; Dardelle et al., 2010; Fry, 2011; Dumont et al., 2014). HG is a polymer consisting of repeating units of (1,4)-α-D-galacturonic acid (GalUA) that is synthesized in the Golgi apparatus and may be deposited in the cell wall in a highly methylesterified form (Zhang and Staehelin, 1992).

Immunolabeling of HG on Arabidopsis pollen tubes showed a dominant localization of the highly methylesterified HG in the tip and of partially methylesterified HG behind the tip region (Dardelle et al., 2010; Chebli et al., 2012). This labeling pattern is also observed in pollen tubes from plants possessing a solid style, such as species in the Solanaceae (potato [*Solanum tuberosum*], tobacco, and petunia [*Petunia hybrida*]), the Oleaceae (jasmine [*Jasmium* spp.]), and the Poaceae (maize [*Zea mays*]; Li et al., 1994; Qin et al., 2007; for review, see Mollet et al., 2013), and those with a hollow style, such as lily (Jauh and Lord, 1996). The methylesterified HG in the apical dome of the pollen tube is thought to provide sufficient plasticity of the cell wall to sustain pollen tube growth (Chebli and Geitmann, 2007). In the subapical region, methylesterified HG is processed by pectin methylesterases (PMEs). Two modes of action have been described for PMEs (Micheli, 2001). If PMEs remove contiguous methylester groups, the mode of action is named the block-wise mode of action. In that case, demethylesterified HG can form ionic bonds between the negatively charged carboxyl groups of several HG chains and Ca^{2+} ions, forming a pectate gel that may provide sufficient stiffness to the pollen tube cell wall (Micheli, 2001; Geitmann and Steer, 2006; Chebli et al., 2012). Alternatively, the partial removal of noncontiguous methylester groups by PMEs, which is named the random mode of action, may allow pectin-degrading enzymes (such as polygalacturonases [PGases] and pectate lyases [PLs]) to cleave the HG backbone, thus affecting the rigidity of the cell wall (Micheli, 2001; Bosch and Hepler, 2005; Parre and Geitmann, 2005a; Sénéchal et al., 2014). Therefore, the fine control of the modulation of the degree of methylesterification (DM) of the HG by PMEs is of main importance (Wolf et al., 2009a) in the pollen tube growth dynamics. The Arabidopsis genome contains 66 putative PMEs. Most of them display a specific expression pattern, especially for 14 of them that are specifically expressed in pollen grains or pollen tubes (Qin et al., 2009; Wolf et al., 2009a). PMEs are classified in two distinct groups depending on the presence/absence of an N-terminal extension domain (the PRO region) showing similarity with the pectin methylesterase inhibitor (PMEI) domain (Micheli, 2001). PMEs from group 1 do not have a PMEI domain but can be inhibited by PMEIs (Röckel et al., 2008), whereas PMEs from group 2 can contain from one to three PMEI domains (Tian et al., 2006). It is hypothesized that the PRO region is cleaved during maturation of the PME, as so far, only PMEs lacking this domain were found in the cell wall (Micheli, 2001). Wolf et al. (2009b) have shown that the PRO region of the group 2 PMEs could regulate the release of the mature PME from the Golgi apparatus. It has also been reported that the PRO region could play an autoinhibitory role during maturation (Bosch et al., 2005).

The first direct evidence for the crucial roles of PMEs during pollen tube growth was described in two knockout mutants, *vanguard1* (*vgd1*; Jiang et al., 2005) and *Atppme1* (Tian et al., 2006). *VGD1* (At2g47040) encodes a pollen-specific group 2 PME. The functional disruption of *VGD1* resulted in the bursting of pollen tubes in vitro and the marked retardation of *vgd1* pollen tube elongation in the pistil, resulting in a strong reduction of male fertility and seed set. *AtPPME1* (At1g69940), coding for a pollen-specific group 1 PME, also was identified to play an important role in pollen tube growth (Tian et al., 2006). The lack of *AtPPME1* transcripts in the knockout mutant affected the shape and growth rate of pollen tubes, indicating that AtPPME1 is required for the integrity of the cell wall and the tip-polarized growth of the pollen tube (Tian et al., 2006).

Here, we report the study of a homozygous knockdown mutant for *AtPME48* during the imbibition and germination of pollen grains and pollen tube growth. We have investigated in vitro and in vivo pollen germination, pollen tube morphology and growth, as well as the level of PME activity and the DM of the HG by immunolabeling and Fourier transform infrared (FT-IR) spectroscopy in mutant and wild-type plants. Our results show that the group 1 PME48, the second most expressed *PME* gene in pollen, plays a major role in remodeling the HG of the intine cell wall during Arabidopsis pollen grain maturation, resulting, after rehydration, in normal pollen grain germination.

RESULTS

Expression of Pollen-Specific PMEs Assessed by Quantitative Reverse Transcription-PCR

The expression of the 14 pollen-specific PME genes was analyzed by quantitative reverse transcription (qRT)-PCR on total RNA extracted from dry and imbibed (for 1 h in liquid germination medium [GM]) pollen grains and 6-h-old pollen tubes. Most PME genes were expressed in dry pollen grains, with a strong expression of PME4 (VGD1 homolog), PME5 (VGD1), PME37, and PME48 (Fig. 1A). During imbibition and in in vitro-grown pollen tubes, PME4, PME5, PME50, as well as PME48 were strongly expressed compared with the 10 other PMEs (Fig. 1, B and C). PME48 and PME50 belong to the group 1 PMEs, whereas PME4 and PME5, known as VGD1 homolog and VGD1 (Jiang et al., 2005), belong to the group 2 PMEs.

Tissue-Specific Expression of *AtPME48*

In order to check whether *PME48* is specifically expressed in pollen, the activity of the promoter of *PME48* was assessed using the *pPME48*::*GUS* and *pPME48*::*YFP* constructs. Fluorescence of the yellow fluorescent protein (YFP) was observed in dry (Fig.

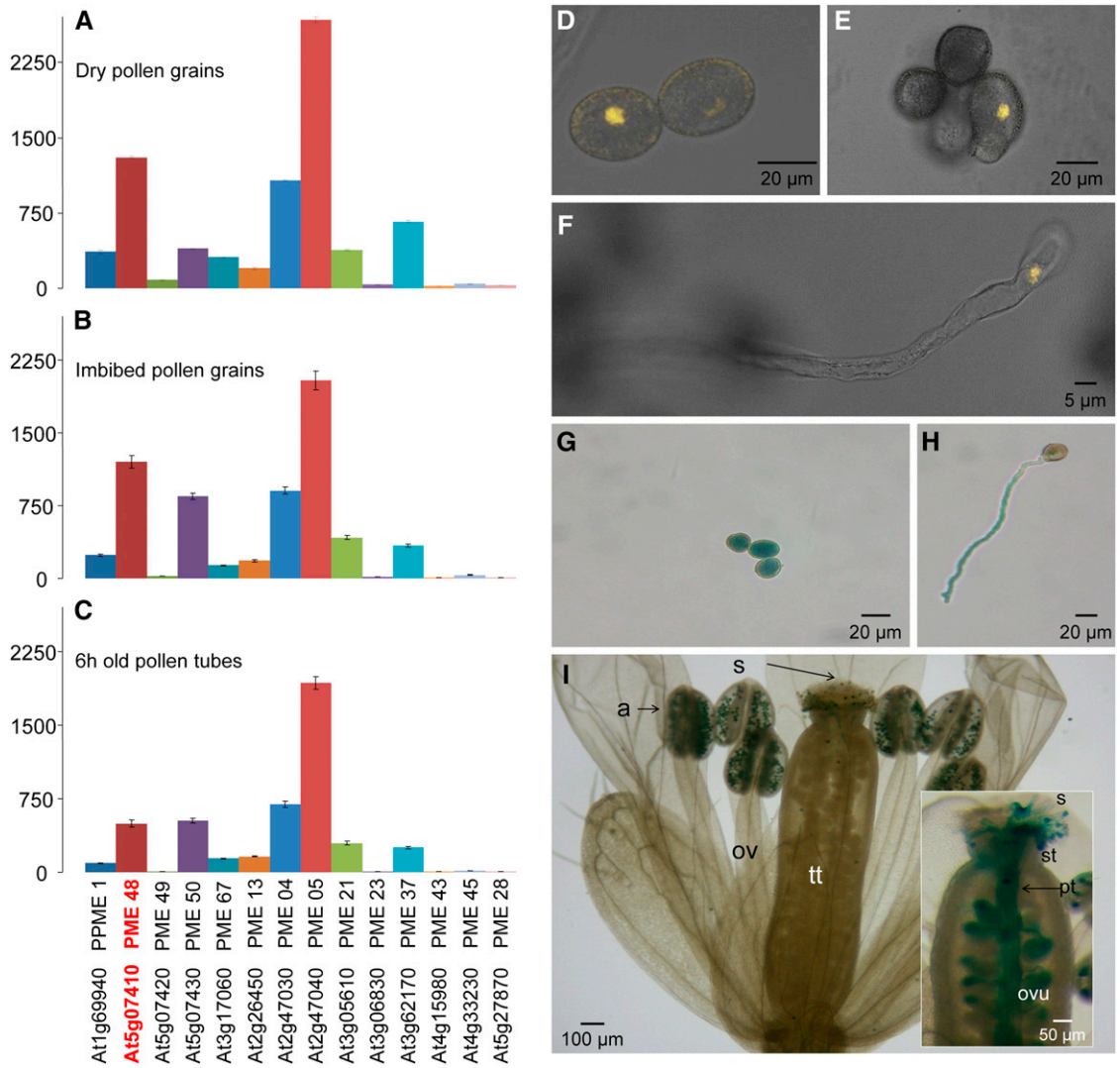

Figure 1. A to C, Relative gene expression of the 14 pollen-specific *PMEs* in wild-type dry pollen grains (A), 1-h imbibed pollen grains (B), and 6-h-old pollen tubes (C) measured using stably expressed reference genes (At3g28750, At3g57690, and At5g59370) in three biological samples with similar results. Only the results obtained with At3g28750 are shown. The locus and the corresponding UniProt name of each protein are indicated. The data correspond to means ± SD of three technical replicates of a biological sample. D to F, Analyses of the expression of the promoter of *PME48* using the *pPME48*::YFP construct by confocal microscopy in dry pollen grains (D), 1-h imbibed pollen grains (E), and during pollen tube growth (F). Images shown are overlays of the bright-field and fluorescent images. G to I, Analyses of the expression of the promoter of *PME48* using the *pPME48*::GUS construct in dry pollen grains (G), 3-h-old pollen tube (H), anthers (I), and self-pollinated pistil (inset in I). a, Anther; ov, ovary; ovu, ovule; pt, pollen tube; s, stigma; st, style; tt, transmitting tract.

1D) and imbibed (Fig. 1E) pollen grains and in 6-h-old in vitro-grown pollen tubes (Fig. 1F). GUS staining showed that the promoter activity of *PME48* was restricted to the male gametophyte (Fig. 1, G–I). GUS activity was detected in dry pollen grains (Fig. 1G) and in 6-h-old in vitro-grown pollen tubes (Fig. 1H). In vivo staining also showed a strong GUS activity in pollen grains within the anther and in germinated pollen grains deposited on the stigma (Fig. 1I). GUS staining was also clearly visible in pollen tubes growing through the transmitting tract (Fig. 1I, inset). Staining was observed neither in the vegetative organs of the transformed plants nor in pollen grains or pollen tubes from wild-type plants (data not shown).

Isolation and Characterization of the *pme48*−/− Homozygous Mutant Line

We selected a transfer DNA (T-DNA) insertion line from the Salk library. SALK_122970 contained a T-DNA insert in the *PME48* coding sequence. The T-DNA insertion was predicted to be located in the last exon of the sequence (Supplemental Fig. S1A). The homozygous

mutant line (*pme48−/−*) has been isolated, two copies of the insert were amplified with the genomic DNA (Supplemental Fig. S1B), and the *PME48* transcript was not detectable by reverse transcription (RT)-PCR (Supplemental Fig. S1C). The vegetative organs of *pme48−/−* did not display any visible phenotype or growth defect compared with wild-type plants (data not shown).

The level of the *PME48* transcript was then analyzed by qRT-PCR in dry, imbibed pollen grains and 6-h-old pollen tubes. Unlike the data obtained by RT-PCR (Supplemental Fig. S1C), qRT-PCR revealed that *pme48−/−* was not a knockout but a knockdown mutant (Fig. 2). *PME48* was lightly expressed in dry (9%; Fig. 2A) and imbibed (10%; Fig. 2B) pollen grains and in 6-h-old pollen tubes (19%; Fig. 2C) compared with wild-type pollen grains and pollen tubes. 4′,6-Diamidino-2-phenylindole (DAPI) staining showed that *pme48−/−* pollen grains contained the two sperm cells and the vegetative nucleus as observed in wild-type pollen grains (Supplemental Fig. S2A). Using fluorescein diacetate (FDA), the viability assays showed that most *pme48−/−* pollen grains were viable (72.3% ± 3.7%), but slightly less than wild-type pollen grains (79% ± 4.6%; $P < 0.0001$, $n > 1{,}000$ for each sample; Supplemental Fig. S2, B and C). In addition, the length of wild-type dry pollen grains was also slightly higher (29.8 ± 0.15 μm) than that of *pme48−/−* pollen grains (28.8 ± 0.12 μm; $P < 0.0001$, $n = 550$ for each sample; Supplemental Fig. S2, D and E). Similarly, the length of the siliques of the mutant was 1.4 mm shorter than that of the wild type ($P < 0.0001$, $n = 210$ for each sample; Supplemental Fig. S2F). The silique of the mutant contained a reduced number of seeds (40.3 ± 1.33 seeds per silique) compared with the wild-type silique (48.6 ± 0.5 seeds per silique; $P < 0.0001$, $n = 210$ for each sample; Supplemental Fig. S2G).

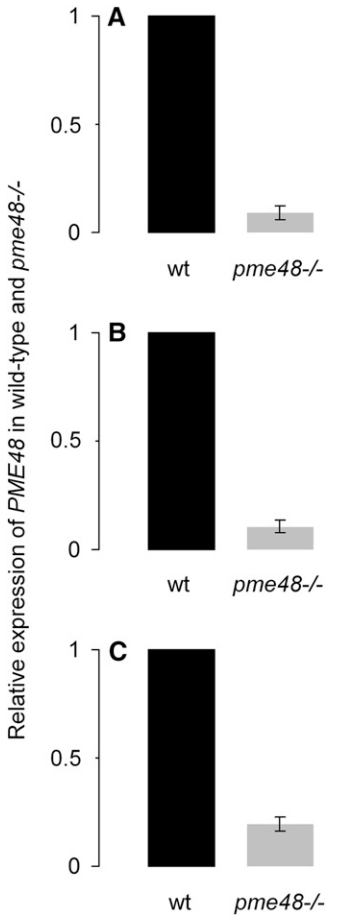

Figure 2. Relative gene expression of *PME48* in *pme48−/−* dry pollen grains (A), 1-h imbibed pollen grains (B), and 6-h-old pollen tubes (C) was measured using stably expressed reference genes (At3g28750, At3g57690, and At5g59370) in three biological samples with similar results. Only the results obtained with At3g28750 are shown. The data correspond to the ratio of expression in the wild type (wt) or *pme48−/−* compared with the wild type and are means ± SD of three technical replicates of a biological sample.

In Vitro and in Vivo Pollen Grain Germination and Pollen Tube Growth of *pme48−/−*

In the optimal solid GM described by Boavida and McCormick (2007), 65% and 90% of wild-type pollen grains were germinated after 6 and 24 h of culture, respectively (Fig. 3A). In contrast, the percentage of germinated *pme48−/−* pollen grains was reduced drastically, as only 10% of the pollen grains were germinated after 24 h of culture ($P < 0.0001$, $n > 10{,}000$ for each sample; Fig. 3A). In liquid medium, 71% and 73% germination was observed after 6 and 24 h of culture for the wild-type pollen grains (Supplemental Fig. S3A). In contrast, the level of *pme48−/−* pollen grain germination did not exceed 43.8% after 6 h of culture and reached only 60% after 24 h ($P < 0.0001$, $n > 10{,}000$ for each sample; Supplemental Fig. S3A). As *pme48−/−* pollen grains displayed a delay in germination, the speed of imbibition of the pollen grains was assessed by calculating the ratio of length to width. Dry pollen grains have ellipsoid shapes, and the length is approximately twice as much as the width. During imbibition, pollen grains become spherical and the length is nearly equal to the width; the length:width ratio is then approximately 1. On the optimal solid medium, the imbibition was faster for the wild-type pollen grains compared with the mutant. The smallest ratio was obtained after 24 h, with 1.16 and 1.39 for the wild-type and *pme48−/−*, respectively (Fig. 3B). After 24 h of culture, pollen grains from the mutant lines were less imbibed than the wild-type pollen grains imbibed for 6 h ($P < 0.0001$, $n > 500$ for each sample). The same result was observed in liquid medium ($P < 0.0001$, $n > 500$ for each sample; Supplemental Fig. S3B). Based on these observations, it appeared that the ability of the pollen grain to rehydrate was affected in *pme48−/−* mutant lines. The delay in germination was also observed in vivo. Hand pollination of emasculated wild-type pistils with wild-type or *pme48−/−* pollen grains showed that the wild-type

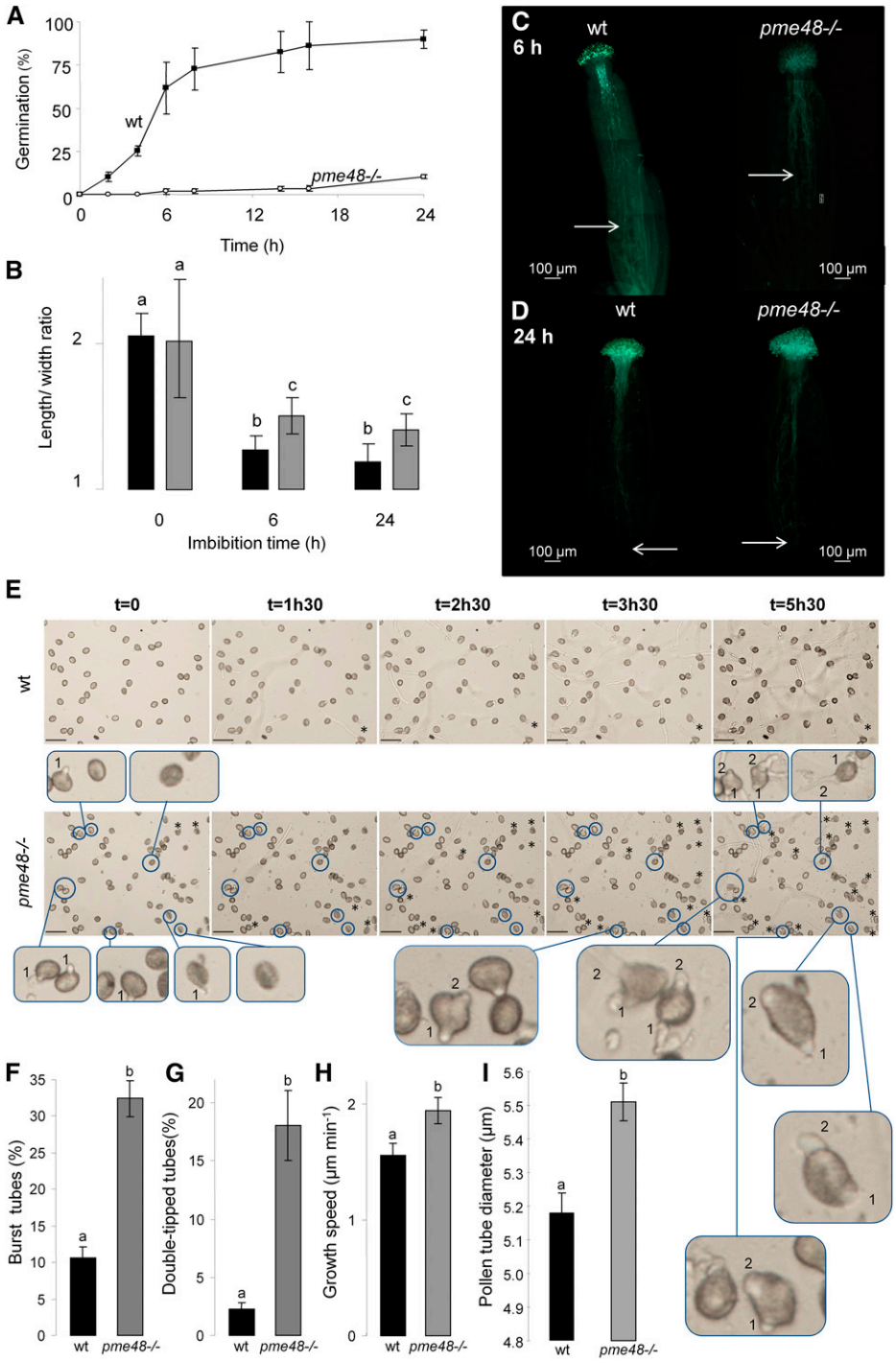

Figure 3. In vitro and in vivo germination of wild-type and *pme48−/−* pollen grains. A, Germination rate of wild-type (wt; black squares) and *pme48−/−* (white circles) pollen grains in the optimum solid medium. Pollen grains were considered germinated when the length of the tube was equal to the diameter of the pollen grain. B, Estimation of the imbibition rate by measuring the ratio of length to width of wild-type (black bars) and *pme48−/−* (gray bars) pollen grains. C and D, In vivo growth of wild-type and *pme48−/−* pollen tubes in wild-type pistil at 6 h (C) and 24 h (D) after hand pollination revealed by Aniline Blue staining. Arrows indicate the locations that most of the pollen tubes have reached in the transmitting tissue. Bars = 100 μm. E, Time-lapse images of wild-type and *pme48−/−* pollen germination in liquid medium showing two emerging tips from the pollen grain (blue circles) and burst tubes (asterisks). Numbers in the closeup images indicate which tubes emerged first. Closeup images of abnormal phenotypes were observed in the mutant line compared with the wild type. Bars = 50 μm. F, Estimation of the rate of burst pollen tubes in the wild type (black bar) and *pme48−/−* (gray bar). G, Estimation of the rate of pollen grains with two emerging tips in the wild type (black bar) and *pme48−/−* (gray bar). H, Estimation of the growth speed of wild-type (black bar) and *pme48−/−* (gray bar) germinated pollen tubes. I, Comparison of the pollen tube diameters between the wild type (black bar) and *pme48−/−* (gray bar) grown in liquid GM for 4 h. Different letters indicate statistically significant differences between the wild-type and *pme48−/−* lines, as determined by Student's *t* test ($P < 0.0001$); $n >$ 10,000 in A; $n > 500$ in B, F, and G; $n > 35$ in H; $n = 126$ for the wild type and $n = 172$ for *pme48−/−* from four independent experiments in I.

pollen tubes had traveled two-thirds of the transmitting tract after 6 h (Fig. 3C, left) and completed their journey by reaching the bottom of the ovary after 24 h (Fig. 3D, left). In contrast, *pme48−/−* pollen tubes had reached only one-half of the transmitting tract after 6 h (Fig. 3C, right), but after 24 h, *pme48−/−* pollen tubes also had reached the base of the ovary (Fig. 3D, right).

In addition to lower germination rates, *pme48−/−* displayed a remarkable phenotype, as shown on the representative images obtained by time-lapse video during the germination of pollen grains and the growth of pollen tubes (Fig. 3E). Wild-type pollen grains had already germinated 90 min after immersion in the liquid medium (Fig. 3E, top), the proportion of burst tubes was around 10% (Fig. 3F), the growth rate was about 1.5 μm min^{-1} during the first 90 min of growth (Fig. 3H; Supplemental Fig. S4), and pollen tubes displayed a normal phenotype (Fig. 3E; Supplemental Movie S1).

On the other hand, *pme48−/−* pollen tubes appeared to be more unstable, with 32% of burst tubes ($P < 0.0001$, $n > 500$ for each sample; Fig. 3F). Moreover, a significant number of *pme48−/−* pollen grains (18%) displayed two tips emerging from the same pollen grain ($P < 0.0001$, $n > 500$ for each sample; Fig. 3, E and G, bottom closeup images). The first tip emerged from pollen grains, and after 4 to 5 h of culture, a second tip emerged from the same pollen grain (pollen grains circled in blue; Fig. 3E, bottom closeup images; Supplemental Movie S2). Once germinated and if pollen tubes were produced, the growth speed of *pme48−/−* pollen tubes was slightly faster compared with wild-type pollen tubes ($P < 0.0001$, $n > 35$ for each sample; Fig. 3H; Supplemental Fig. S4). Another consequence of the *PME48* mutation was that pollen tubes growing in liquid GM displayed larger diameters than wild-type pollen tubes (Figs. 3I and 4, A and H). The *pme48−/−* pollen tube diameters were significantly wider (5.51 ± 0.05 μm) compared with wild-type pollen tubes (5.18 ± 0.06 μm; $P < 0.0001$, $n = 126$ for wild-type pollen tubes and $n = 172$ for *pme48−/−* pollen tubes; Fig. 3I).

Immunolabeling of Highly Methylesterified HG in Pollen Grains and Pollen Tubes

Cell surface immunolocalization of highly methylesterified HG with the monoclonal antibody LM20 revealed that the epitopes were almost exclusively restricted to the tip region of wild-type pollen tubes (Fig. 4, A–E). Pollen grains from wild-type plants showed a very weak, almost no, labeling of the intine wall (Fig. 4, C–E). Similar results were obtained on semithin sections (Fig. 4, F and G). In contrast, the labeling of *pme48−/−* pollen tubes was not restricted to the tube tip but extended to the subapical region of the tube, but with the strongest fluorescence at the tip (Fig. 4, H–K). Finally, *pme48−/−* pollen grains displayed a more intense fluorescence of the intine wall by cell surface immunolabeling (Fig. 4, J–L) and on semithin sections (Fig. 4, M and N) compared with the wild type.

Immunolabeling with the monoclonal antibody LM19 that recognizes weakly methylesterified HG epitopes did not reveal any noticeable difference between the wild type and *pme48−/−* (data not shown). LM19 and LM20 show overlapping binding capabilities to different levels of methylesterification, except for totally deesterified HG epitopes that are only recognized by LM19 (Verhertbruggen et al., 2009). Therefore, these results suggest that highly methylesterified HG epitopes were more abundant in the intine wall of *pme48−/−* pollen grains compared with the wild type.

PME Activity and DM of HG in *pme48−/−*

In order to assess further the biochemical differences between the wild type and *pme48−/−*, we investigated the total PME activity in pollen grains by using enzymatic assays. The data showed a 50% reduction of total PME activity in *pme48−/−* pollen grains compared with the wild type (Fig. 5A). Moreover, a zymogram after isoelectric focalization (IEF) of total proteins extracted from pollen grains revealed the disappearance of a diffuse band in the pI range between 8.2 and 9 in *pme48−/−* (Fig. 5B) that may correspond at least in part to PME48, which has a predicted pI of 8.3. Two spots, at pI ranging from 9.8 to 10.2 and from 9.5 to 9.7, in the range of predicted pIs of other pollen PMEs did not show any visible change in activity (Fig. 5B). These

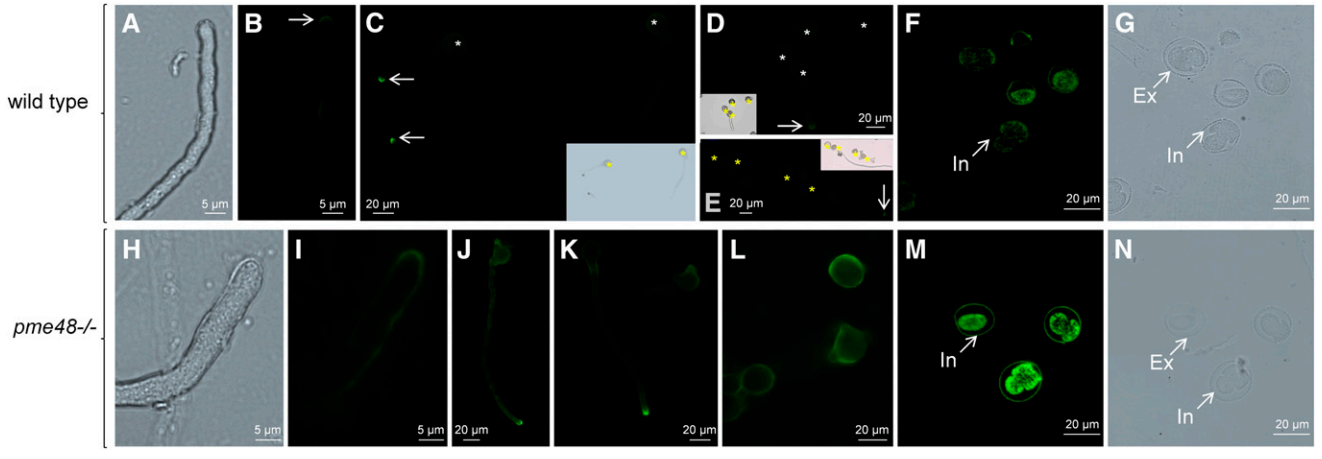

Figure 4. Immunolocalization of highly methylesterified HG epitopes probed with LM20 in wild-type and *pme48−/−* pollen grains and pollen tubes. A to E, Cell surface immunolabeling in wild-type pollen grains and pollen tubes. F and G, Immunolabeling on semithin sections of wild-type dry pollen grains. H to L, Cell surface immunolabeling in *pme48−/−* pollen grains and pollen tubes. M and N, Immunolabeling on semithin sections of *pme48−/−* dry pollen grains. Asterisks indicate pollen grains, and arrows point to pollen tube tips. Ex, Exine; In, intine.

biochemical data support the qRT-PCR results that clearly showed a significant reduction of *PME48* expression. Finally, the DM of HG was estimated by FT-IR spectroscopy in hot water-soluble pectin-enriched fractions extracted from dry pollen grains (Fig. 5, C and D). A marked difference was observed at 1,740 cm^{-1} assigned to the vibration of methylester groups of HG (Fig. 5C). The relative absorbance at this wave number was higher in *pme48−/−* pollen grains. The DM of the HG was consistently higher in the *pme48−/−* (32.5% ± 1.7%) compared with the wild-type (13.4% ± 1.1%) pollen grains (Fig. 5D). As deesterified HG binds more Ca^{2+} than esterified HG, our data may suggest that HGs in the intine wall of *pme48−/−* are less associated with Ca^{2+} compared with wild-type pollen grains.

Supplementation of Ca^{2+} to the GM Restores the Phenotype of *pme48−/−*

To assess if the germination defect of *pme48−/−* pollen grains was related to the possible lower Ca^{2+} sink in the intine wall due to the higher DM of the HG, the optimum culture medium containing 5 mM $CaCl_2$ was supplemented with 2.5 mM $CaCl_2$ to reach a final concentration of 7.5 mM or with the Ca^{2+} chelator, EDTA. In the presence of 1 mM EDTA, none of the wild-type and *pme48−/−* pollen grains germinated, even after 24 h of culture ($n > 1,000$; Fig. 6, A and B). In the medium supplemented with Ca^{2+}, *pme48−/−* pollen grain germination rates were restored, reaching levels similar to those observed with wild-type pollen grains ($n > 1,000$). The percentage of pollen germination reached 52% and 90% after 6 and 24 h, respectively (Fig. 6, A and B). Moreover, the speed of imbibition of *pme48−/−* pollen grains was as fast as that of the wild-type pollen grains (Fig. 6C). In addition, a significant reduction of the abnormal phenotypes, such as burst tubes (from 33% to 13%; Figs. 3F and 6D) and double-tipped tubes (from 18% to 2%; Figs. 3G and 6E), was observed in *pme48−/−* pollen grains cultured in the supplemented GM. Finally, in the $CaCl_2$-supplemented medium, the rates of burst tubes increased in wild-type pollen grains (32%; Fig. 6D) compared with those observed when pollen grains were grown in the optimum GM (approximately 10%; Fig. 3F).

DISCUSSION

The regulation of the DM of HG has been implicated in many aspects of plant development (Wolf et al., 2009a), including cell adhesion (Tieman and Handa, 1994; Wen et al., 1999; Mollet et al., 2000; Bouton et al., 2002; Mouille et al., 2007; Durand et al., 2009), adventitious rooting (Guénin et al., 2011), primordia emergence at the shoot apical meristem (Peaucelle et al., 2008, 2011), fruit ripening (Brummell and Harpster, 2001; Phan et al., 2007), and plant defense (Bethke et al., 2014). Although data have shown an important role for

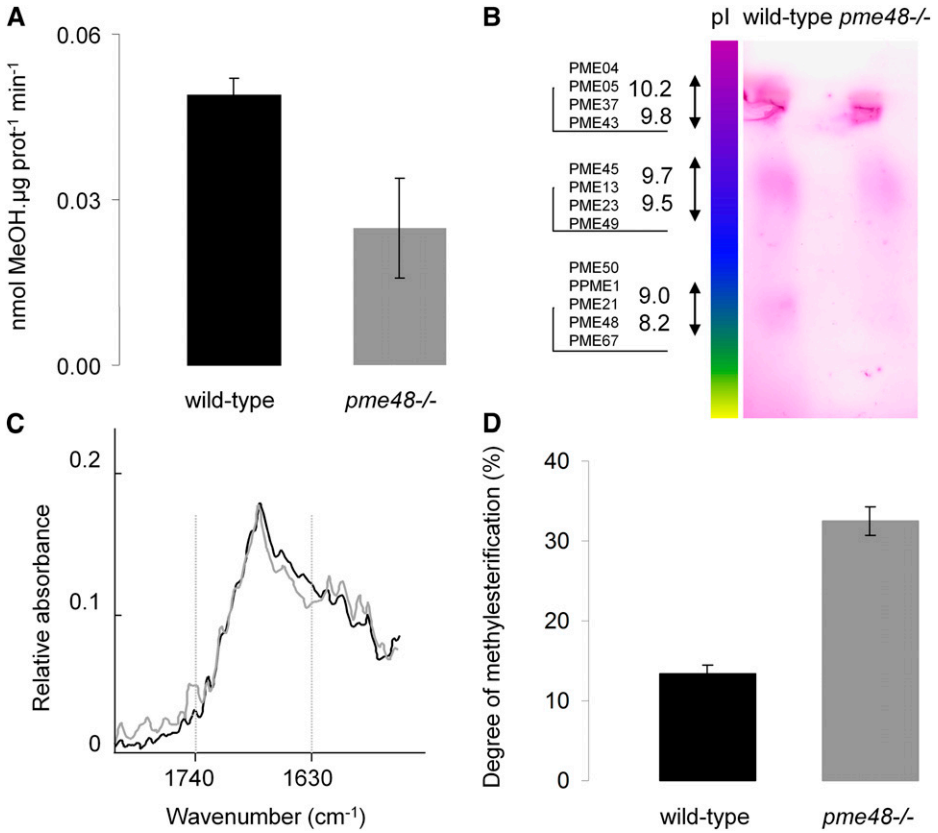

Figure 5. Biochemical analyses of wild-type and *pme48−/−* dry pollen grains. A, Enzymatic assay of the total PME activity contained in wild-type (black bar) and *pme48−/−* dry (gray bar) pollen grains. MeOH, Methanol. B, Zymogram after IEF of PMEs contained in wild-type and *pme48−/−* dry pollen grains. A diffuse band corresponding to the pI (8.2) of PME48 is lacking in *pme48−/−* dry pollen grains. C and D, Determination of the DM of the HG in dry pollen grains by FT-IR spectroscopy. C, Representative FT-IR spectra of pectin-enriched fractions extracted from wild-type (black trace) and *pme48−/−* (gray trace) dry pollen grains. D, Quantification of the DM of HG in wild-type (black bar) and *pme48−/−* (gray bar) pollen grains. Data are means of three biological replicates ± SD.

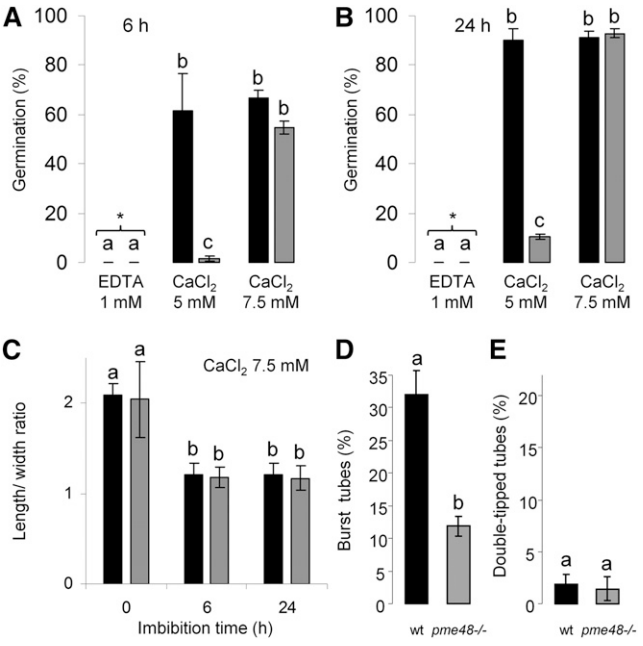

Figure 6. Effect of calcium on the germination and phenotype of pollen tubes. A and B, Germination percentage of wild-type (black bars) and *pme48−/−* (gray bars) pollen grains in the optimal solid medium (5 mM $CaCl_2$), in the optimal solid medium supplemented with 1 mM EDTA, and in the optimal medium supplemented with 2.5 mM calcium (i.e. final concentration of $CaCl_2$, 7.5 mM) after 6 h (A) and 24 h (B) of growth. Pollen grains were considered germinated when the length of the tube was equal to the diameter of the pollen grain. C, Estimation of the imbibition rate by measuring the ratio of length to width of wild-type (black bars) and *pme48−/−* (gray bars) pollen grains in the solid medium containing 7.5 mM $CaCl_2$. D, Estimation of the rate of burst pollen tubes in the wild type (wt; black bar) and *pme48−/−* (gray bar) in solid medium containing 7.5 mM $CaCl_2$. E, Estimation of the rate of pollen grains with two emerging tips in the wild type (black bar) and *pme48−/−* (gray bar) in solid medium containing 7.5 mM $CaCl_2$. Different letters indicate statistically significant differences between the wild-type and *pme48−/−* lines, as determined by Student's *t* test ($P < 0.0001$); $n > 1{,}000$ in A and B; $n > 500$ in C; and $n > 250$ in D and E.

the pectin demethylesterification process in pollen tetrad separation (Francis et al., 2006) and pollen tube growth (Jiang et al., 2005; Tian et al., 2006), the involvement of PMEs during pollen germination is still poorly understood. Among the 66 predicted *PME* genes in the genome of Arabidopsis, 14 are specifically expressed in the male gametophyte (data from Genevestigator [Hruz et al., 2008] and EFP Browser [Winter et al., 2007]). Two of them have already been studied using functional genomics approaches. The first one is VGD1 (At2g47040), the alteration of which led to unstable pollen tubes and retarded growth of the pollen tube in the style and transmitting tract, resulting in a significant reduction of male fertility (Jiang et al., 2005). The second pollen-specific PME characterized to date is PPME1 (At1g69940; Tian et al., 2006). The homozygous mutant *Atppme1* displayed reduced growth and irregular shape of pollen tubes grown in vitro. In this study, we show that alteration of the expression of *PME48*, the second most expressed *PME* in pollen grains, results in a strong delay in imbibition and in germination both in vivo and in vitro, as well as altered phenotypes with abnormal rates of burst tubes and two pollen tube tips emerging from the same pollen grain. The phenotype is rescued by supplementing the optimum GM (Boavida and McCormick, 2007) with 2.5 mM $CaCl_2$ to reach 7.5 mM. In 7.5 mM $CaCl_2$, *pme48−/−* pollen grains imbibed and germinated normally. These data suggest that PME48 is mainly involved in the remodeling of the intine cell wall during maturation of the pollen grain. The reduction of PME48 activity also has consequences later on pollen tube morphology. The pollen tubes are slightly wider in the mutant, which may reflect the role of HG in the mechanical properties of the cell wall (Parre and Geitmann, 2005a; Palin and Geitmann, 2012) and corroborates the predictions made by mechanical simulations (Chebli and Geitmann, 2007; Zerzour et al., 2009; Fayant et al., 2010). The more abundant highly methylesterified HG in the intine wall of *pme48−/−* pollen grains and at the tip and in the subapical region of *pme48−/−* pollen tubes provides more viscoelasticity and less rigidity of the cell wall, thus promoting several tips emerging from the pollen grain and wider diameters of pollen tubes, probably due to the internal turgor pressure (Parre and Geitmann, 2005a; Winship et al., 2010).

Mature pollen grains are surrounded by two cell walls: the outer exine and the inner intine. In many species, such as tobacco (Li et al., 1995), Arabidopsis (Van Aelst and Van Went, 1992; Rhee and Somerville, 1998), *Lilium hybrida* (Aouali et al., 2001), *Euphorbia peplus* (Suárez-Cervera et al., 2002), *Zygophyllum fabago* (Castells et al., 2003), and *Larix decidua* (Rafińska et al., 2014), the intine of mature pollen grains is mostly composed of weakly methylesterified HG or a mix of highly and weakly methylesterified HGs, the latter being more abundant. The almost absent labeling of weakly methylesterified HG with John Innes Monoclonal5 at the pollen mother cell and tetrad stages (Rhee and Somerville, 1998) but its strong detection in the intine at the late microspore stage and mature dry Arabidopsis pollen grains (Van Aelst and Van Went, 1992; Rhee and Somerville, 1998) indicate an early action of PMEs during pollen formation and maturation. HG polymers are synthesized in the Golgi apparatus and may be secreted under a highly methylesterified form and then processed in the cell wall by PMEs (Zhang and Staehelin, 1992; Caffall and Mohnen, 2009; Harholt et al., 2010). This is consistent with our qRT-PCR results showing that pollen-specific PMEs, including *PME48*, are strongly expressed in dry pollen grains. A similar pattern of expression of these *PMEs* was obtained previously in two transcriptomic analyses of dry pollen grains and pollen tubes (Wang et al., 2008; Qin et al., 2009). Moreover, proteomic analyses of Arabidopsis revealed the presence of at least three PMEs in mature pollen grains: PME37, PPME1, and PME48 (Holmes-Davis et al., 2005; Ge et al., 2011). Similarly, at least two PMEs were found in the

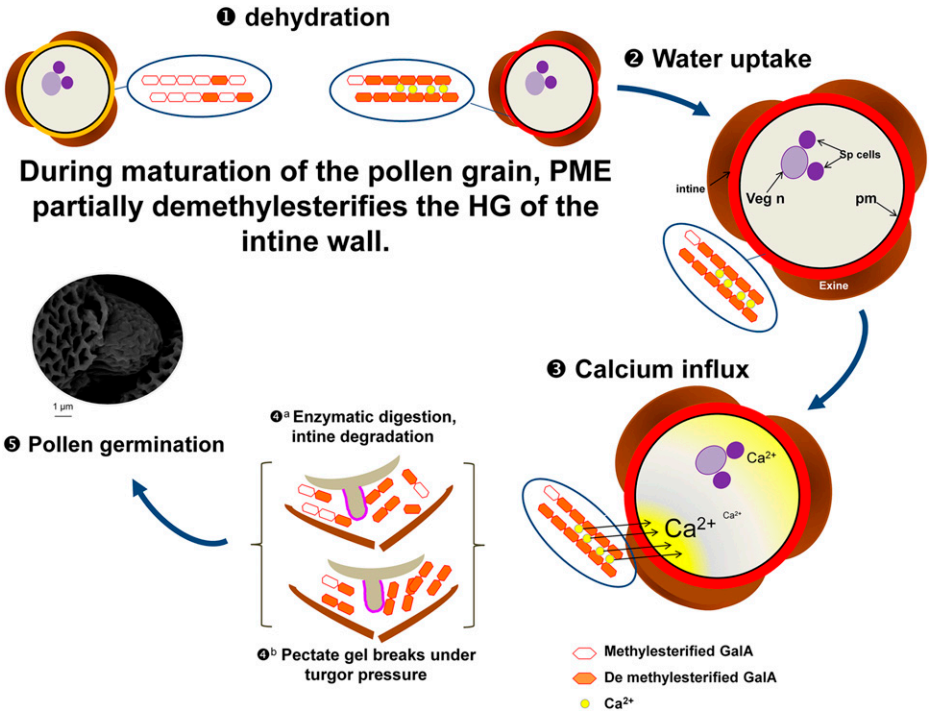

Figure 7. Model showing the possible mode of action of PME48 during pollen dehydration, imbibition, and germination. 1, PME48 may be secreted in the intine wall during the maturation of the pollen grain and start to act on the methylesterified form of the HG by random or block-wise actions. Methylesterified HG of the intine (black) is then transformed in weakly methylesterified HG (orange). The dry pollen grain contains mostly weakly esterified HG that could form pectate gel with calcium. 2, Imbibition of the pollen grain is enhanced by the presence of the more hydrophilic weakly methylesterified HG. 3, The source of calcium creating the calcium influx in the pollen grain may originate, at least partially, from the release of Ca^{2+} from the pectate gel, thus weakening the mechanical properties of the intine. 4, The intine may be degraded by PGases and/or PLs (a) and/or break under the turgor pressure (b). 5, These processes may promote the emergence of the pollen tube tip and allow the germination of the pollen grain. GalA, (1,4)-α-D-GalUA; pm, plasma membrane; Sp, sperm cells; Veg n, vegetative nucleus.

proteome of rice (*Oryza sativa*; Dai et al., 2006) and maize (Zhu et al., 2011) dry pollen grains.

The early demethylesterification of HG by PME48 during pollen formation and maturation (Fig. 7) may have three major consequences. First, the removal of hydrophobic methylester groups can enhance the hydrophilic properties of the cell wall, thus promoting pollen grain hydration (Fig. 7). The DM of HG can affect the water-holding capacity of the pectate gel (Willats et al., 2001), leading to water loss and changes of the physical properties of the pectate gel, which appeared to collapse under pressure (Willats et al., 2001). The *mucilage modified2* (*mum2*) mutant (impaired in the expression of a β-galactosidase) failed to properly hydrate the seed mucilage (Macquet et al., 2007). Interestingly, in the mucilage of *mum2*, the content of methylesterified HG increased compared with the wild type, suggesting that (1) β-galactosidase may be required for PME activity (Western et al., 2001; Walker et al., 2011) and (2) PME activity is required for the hydration of HGs. This observation may explain why, in the *pme48−/−* mutant lines, the imbibition and germination of pollen grains were strongly delayed, as the DM of the HG in the intine of *pme48−/−* is almost 2.5-fold higher than in the wild type. Second, upon the block-wise action of PMEs, deesterified blocks of HG chains can be cross-linked with calcium (Micheli, 2001). During wild-type pollen grain formation and maturation, the activity of PME48 promotes the release of negative charges of the carboxylic groups, allowing the interaction of calcium with the HG chains. The main Ca^{2+} sink in the plant cell wall is the demethylesterified HG (Wolf et al., 2009a; Hepler et al., 2012). Thus, the unesterified HG in the maturing pollen grain may act as a reservoir of Ca^{2+} that will be used later during rehydration and germination (Fig. 7). The reduction of PME activity in *pme48−/−* may locally affect the binding capacity of calcium ions by HGs. This possibly may explain the reverse phenotype observed in the calcium-supplemented GM. In vitro pollen germination of many species requires Ca^{2+} (Brewbaker and Kwack, 1963; Ge et al., 2007), and Ca^{2+} plays a central role during pollen germination (Brewbaker and Kwack, 1963; Ge et al., 2007; Hepler et al., 2012), acting putatively as a signal to activate the germination process and/or acting directly on the physical property of the intine. Ca^{2+} dynamics have been investigated in Arabidopsis pollen grains during germination (Iwano et al., 2004).

Those authors have shown that, during pollen grain hydration, cytoplasmic Ca^{2+} increased at the future site of protrusion of the pollen tube tip but not exclusively, as, often, an increase also was observed at the opposite site (Fig. 7). The early action of PME48 during the maturation and dehydration of pollen grains and the accumulation of Ca^{2+} in the intine may help to prepare the future protrusion of the pollen tube tip by weakening the intine wall (Fig. 7). Recently, Rafińska et al. (2014) suggested that the cell wall of the female tissues also can act as a reservoir of Ca^{2+} in order to ensure correct germination and pollen tube growth in *L. decidua*. Upon pollination, an increase of Ca^{2+} concentration also was observed in the stigma and transmitting tract of lily (Zhao et al., 2004) and tobacco (Ge et al., 2009). This observation may explain why the impact of the *PME48* mutation on in vivo pollen germination and tube growth was not as dramatic as that in vitro in the optimum solid GM. However, we cannot rule out that PMEs originating from the stigma also may participate in this process or that pollen grains cultured in in vitro and semi-in vivo conditions display a different gene expression pattern (Qin et al., 2009).

As discussed by Jolie et al. (2010), the pH, the DM, and the pattern of methylesterification are known to modify the mode of action of PMEs (Catoire et al., 1998; Denès et al., 2000; Sénéchal et al., 2014). Thus, we can also hypothesize that, upon random action of the PME (PME48 or others from the 13 other pollen-specific PMEs), the partial removal of methylester groups may allow other pectin-degrading enzymes such as PGases and/or PLs to cleave the HG, affecting the rigidity of the cell wall (Micheli, 2001; Sénéchal et al., 2014). In the Arabidopsis genome, 69 annotated genes can be classified as putative PGases (González-Carranza et al., 2007). A semiquantitative RT-PCR analysis investigating 66 among the 69 genes coding for PGases showed that 32 genes were strongly expressed in flower tissues (Kim et al., 2006). Other studies also have shown that PGases were present in ungerminated pollen grains of *Brassica napus* (Dearnaley and Daggard, 2001) and during hydration of *Platanus acerifolia* pollen grains (Suárez-Cervera et al., 2005). In addition, in *Brassica campestris*, alteration of the expression of *B. campestris MALE FERTILITY2* (coding for a putative PGase) resulted in an overdeveloped intine and abnormal germination (Huang et al., 2009). The transcriptome analysis of Arabidopsis pollen grains has revealed that six genes coding for putative PGases and four genes encoding putative PLs are strongly expressed in dry pollen grains and pollen tubes (for review, see Mollet et al., 2013). Taken together, these observations suggest that the early action of PME48 during maturation of the pollen grain also may be required to ensure the future degradation of the intine by PGases and PLs (Fig. 7). Enzymes originating from the stigma also may participate in the degradation of HGs in the intine. Such enzymes, including PGases, have been found in the exudates from lily and olive (*Olea europaea*) stigmas (Rejón et al., 2013).

Although pollen-specific PMEs are traditionally associated with pollen tube elongation, this study provides substantial evidence that PMEs, especially PME48, also are directly implicated in changes of the mechanical properties of the intine wall during maturation, promoting the correct germination of mature pollen grains.

MATERIALS AND METHODS

Plant Materials, Growth Conditions, and Mutant Genotyping

Arabidopsis (*Arabidopsis thaliana* ecotype Columbia-0) wild-type and mutant seeds, stored at 4°C, were spread on the surface of sterile soil and cultured in a growth chamber with a photoperiod of 16 h of light/8 h of dark at 20°C during the light phase and at 16°C in the dark phase with 60% humidity with daily watering.

pme48−/− (mutant of the *PME48* gene; At5g07410) seeds originated from the Arabidopsis Biological Resource Center and corresponded to SALK_122970 (T-DNA 1,403 bp downstream of ATG). Homozygous plants for the T-DNA insertion in the *PME48* gene were identified by PCR. Genotyping PCR was performed with primer pair PME48-F1 (5′-TGACAAGACCGTGTTCTACG-3′)/PME48-R1 (5′-GAAGAGAGGATTTCTGGAAATTGA-3′) and LB (5′-GCGTGGACCGCTTGCTGCAACT-3′) matching with the left border of the T-DNA.

qRT-PCR Analyses

Gene Expression of Pollen-Specific PMEs

Total RNA was extracted from pollen of 6-week-old wild-type and *pme48−/−* plants using the NucleoSpin RNA Plant Kit (Macherey-Nagel) as described by the supplier. After RNA quantification using NanoDrop spectrophotometry and a DNase treatment, 100 ng of RNA was converted into single complementary DNAs (cDNAs) with the QuantiTect Reverse Transcription Kit (Qiagen) following the instructions of the supplier.

Real-time quantitative PCR analyses were performed on 1:5 diluted cDNA. For real-time quantitative PCR, the LightCycler 480 SYBR Green I Master (Roche; catalog no. 04887352001) was used on 384-well plates in the LightCycler 480 Real-Time PCR System (Roche). The crossing threshold values for each sample (the number of PCR cycles required for the accumulated fluorescence signal to cross a threshold above the background) were acquired with the LightCycler 480 software (Roche) using the second derivative maximum method. Primers used are shown in Supplemental Table S1. Stably expressed reference genes (At3g28750, At3g57690, and At5g59370), specifically designed for this study on pollen grains, were selected using GeNorm software (Vandesompele et al., 2002). They were used as internal controls to calculate the relative expression of target genes according to the method described by Gutierrez et al. (2009). Each amplicon was first sequenced to ensure the specificity of the amplified sequence.

Analysis of PME48 Transcripts in Mutant Lines

The lack of *PME48* transcript in *pme48−/−* was checked by RT-PCR using PME48-F2 (5′-CTGGAACTGGAGGAGGAACT-3′) and PME48-R2 (5′-CATAAATCTCAACTCCTCCATG-3′). PCR was performed on the cDNA generated from total RNA extracted from 6-h-old pollen tubes grown in vitro. Primers used for the RT-PCR are in boldface and underlined in Supplemental Figure S1D.

Analysis of Promoter Activity

GUS Staining

Mutant seeds containing 1 kb of the promoter of At5g07410 upstream of the GUS coding sequence were generated as described by Louvet et al., (2006).

GUS staining was performed on dry pollen grains, in vitro-grown pollen tubes, and in vivo on self-pollinated flowers. Flower and dry pollen grain samples were fixed in cold acetone for 20 min and rinsed three times in 50 mM phosphate buffer, pH 7, containing 2 mM potassium ferricyanide, 2 mM

potassium ferrocyanide, and 0.2% (v/v) Triton X-100. In vitro-grown pollen tube samples were not incubated in acetone. Samples were then incubated for 16 h in the dark at 37°C in 50 mM phosphate buffer, pH 7, containing 1 mM 5-bromo-4-chloro-3-indolyl-β-glucuronic acid, 2 mM potassium ferricyanide, 2 mM potassium ferrocyanide, and 0.2% (v/v) Triton X-100. Flower samples were then cleared with several washes in 70% (v/v) ethanol.

Analysis of the Activity of the Promoter of PME48 Using YFP

The promoter of the PME48 gene (At5g07410) was PCR amplified from a plasmid construct containing this sequence cloned upstream of the GUS coding sequence in the pBI101.3 binary vector (Louvet et al., 2006). A ligation-independent cloning method was used to insert the promoter of the *PME48* gene (*pPME48*) upstream of the super YFP (Kremers et al., 2006) in a ligation-independent cloning binary vector, named pPLV06 (GenBank accession no. JF909459) and belonging to the set of plant ligation-independent cloning vectors made by De Rybel et al. (2011). This vector also contains the Simian Virus40 nuclear localization signal. The PCR-amplified promoter insert contained in the plasmid construct was subsequently verified by sequencing, and the plasmid was used to transform *Agrobacterium tumefaciens* GV3101::pSOUP (Hellens et al., 2000). Arabidopsis plants were transformed by floral dip as described by Zhang et al. (2006) and selected on kanamycin (25 mg L^{-1}).

In Vitro Pollen Tube Growth

Pollen grains were grown in vitro in a liquid medium according to the method described by Boavida and McCormick (2007). Briefly, flowers (40 per 1.5-mL tube) were submerged in 1 mL of GM (pH 7.5) containing 5 mM $CaCl_2$•$2H_2O$, 0.01% (w/v) H_3BO_3, 5 mM KCl, 1 mM $MgSO_4$•$7H_2O$, and 10% (w/v) Suc. Tubes were shaken with a vortex to release the pollen grains from the anthers. Flowers were removed with a pair of tweezers, and the pollen suspension was then centrifuged at 4,000*g* for 7 min. New GM (250 μL) was added to the pellet, and pollen grains were transferred into glass vials (14 × 45 mm) and grown in a growth chamber in the dark at 22°C. For solid medium culture, 1.5% agarose (Sigma) was added to the GM and deposited on a microscope slide. After polymerization, wild-type or mutant open flowers were gently brushed on the surface of the agarose pad to release the pollen grains. Glass slides were then placed in a growth chamber in the dark at 22°C under 100% relative humidity. Before any further manipulation, pollen germination and pollen tube growth were assessed with a microscope.

Twenty images per sample were acquired after 2, 4, 6, 8, 14, 16, and 24 h of culture, and the percentage of germination ($n > 10{,}000$) and the speed of growth of pollen tubes ($n > 35$) were measured using ImageJ software (Abràmoff et al., 2004). Germination assays and the speed of growth of pollen tubes were repeated six times. For measurement of the diameter of pollen tubes, wild-type and *pme48−/−* pollen grains were harvested by dabbing flowers onto silane-coated microscope slides. Slides were incubated at 30°C for 30 min in a moist chamber, subsequently covered with liquid GM, and grown for 4 h in a growth chamber in the dark at 22°C. The diameter of pollen tubes was determined on the images with ImageJ ($n = 126$ and $n = 172$ for wild-type and *pme48−/−* pollen tubes, respectively, from four independent experiments).

Pollen grains were also cultured in the GM supplemented with 1 mM EDTA or 2.5 mM $CaCl_2$•$2H_2O$ to reach the final concentration of 7.5 mM $CaCl_2$.

In Vivo Pollen Tube Growth

Emasculated mature flowers from wild-type plants were hand pollinated with wild-type or mutant (*pme48−/−*) pollen grains. The pollinated pistils were collected 6, 12, and 24 h after pollination and fixed in an ethanol:acetic acid (3:1, v/v) solution. The fixed pistils were rehydrated with successive baths of ethanol (70%, 50%, and 30% [v/v]), washed three times with distilled water, and treated overnight in a softening solution composed of 8 M NaOH. After several washes with distilled water, the pistil tissues were stained with decolorized Aniline Blue solution (0.1% [w/v] Aniline Blue in 100 mM K_3PO_4 buffer, pH 11) for 2 h in the dark (Johnson-Brousseau and McCormick, 2004).

Viability Test and DAPI Staining

The viability of pollen grains was assessed using FDA dissolved in acetone at 10 mg mL^{-1} and stored at −20°C. Prior to each experiment, FDA was diluted in a 10% Suc solution to a final concentration of 0.2 mg mL^{-1}. Hydrated pollen grains were dipped in 250 μL of the FDA solution on a glass slide and kept in the dark for 5 min. A minimum of 1,000 pollen grains were analyzed.

The nuclei of the pollen grains were stained with 10 μg mL^{-1} DAPI for 15 min in the dark at room temperature. At least 250 pollen grains were analyzed for each mutant or the wild type.

Immunolocalization of Highly Methylesterified HG Epitopes

Immunolocalization was performed by cell surface labeling as described previously by Dardelle et al. (2010) or on semithin sections. For the cell surface immunolabeling, pollen grains or pollen tubes in GM were mixed (v/v) with a fixation medium containing 100 mM PIPES buffer, pH 6.9, 4 mM $MgSO_4$•$7H_2O$, 4 mM EGTA, 10% (w/v) Suc, and 5% (w/v) formaldehyde and incubated for 90 min at room temperature. Pollen grains or pollen tubes were rinsed three times by centrifugation with 50 mM PIPES buffer, pH 6.9, 2 mM $MgSO_4$•$7H_2O$, and 2 mM EGTA and three times with phosphate-buffered saline (PBS; 100 mM potassium phosphate, pH 7.4, 138 mM NaCl, and 2.7 mM KCl).

For immunolocalization on semithin sections, dry pollen grains were fixed in ethanol:acetic acid (3:1, v/v) and rinsed in 75% (v/v) ethanol. After centrifugation, the pellet of pollen grains was embedded in a block of 2% (w/v) agarose. The block was then incubated in 75%, 95%, and 100% (v/v) ethanol for 1.5 h each at room temperature. Pollen grains were then transferred in increasing concentrations of methacrylate (25%, 50%, 75%, and 100%) according to Baskin et al. (1992). The resin was polymerized at 4°C for 24 h under UV light. Semithin sections (1 μm) were obtained with the EM UC6 ultramicrotome (Leica) and deposited on poly-L-Lys-coated microscope slides.

Samples were then incubated overnight at 4°C with the LM20 antibody that recognizes methylesterified HG epitopes (Verhertbruggen et al., 2009; diluted 1:5 with PBS + 3% [w/v] milk). Samples were rinsed three times with PBS and incubated for 3 h at 30°C with the secondary antibody, a goat anti-rat IgG (whole molecule)-fluorescein isothiocyanate, diluted 1:100. Controls were carried out by incubation of pollen grains or pollen tubes with the secondary antibody only.

Image Acquisition

Pollen grains and pollen tubes were observed under bright-field and fluorescence illumination on a Leica DLMB microscope equipped with the FDA filter (absorption, 470; emission, 520–560 wavelength) under UV illumination for DAPI and decolorized Aniline Blue staining (absorption, 358; emission, 461 wavelength) or fluorescein isothiocyanate filter (absorption, 490; emission, 520 wavelength). Images were acquired with the Leica DFC300FX camera. Pollen grains and pollen tubes expressing *pPME48::YFP* were observed with a laser scanning confocal microscope (Leica TCS SP2 AOBS). YFP was visualized using the 488-nm laser line of an argon laser with a 510- to 530-nm band-pass filter. Pollen grains were also observed using the Hitachi TM3000 tabletop scanning electron microscope in analytical mode. Time-lapse imaging was performed with the inverted Leica DMI 6000B microscope equipped with the Leica DFC450C camera.

FT-IR Spectroscopy

Eight milligrams of pollen grains from wild-type or mutant plants was collected with the vacuum-pollen method described by Johnson-Brousseau and McCormick (2004). After removing the flower debris with tweezers, pollen grains were placed into microcentrifuge tubes containing 96% ethanol. After several washes, the samples were dried overnight under a fume hood. Pollen grains were then incubated for 1 h in 200 μL of sterilized water at 100°C. After a speed vacuum treatment to eliminate water, samples were oven dried for 48 h to obtain a pectin-enriched fraction. This fraction was stored in a sealed container with silica gel prior to FT-IR analysis. Dry samples were analyzed with an OMNI-Sampler FT-IR spectroscope (version 5.2a) at 4 cm^{-1} resolution. The DM was calculated using the absorbance intensities at 1,630 and 1,740 cm^{-1} assigned to the vibration of carboxyl groups of (1,4)-α-D-GalUA and its methylester form, respectively (Gribaa et al., 2013), using the equation described by Gnanasambandam and Proctor (2000) and Manrique and Lajolo (2002): $DM = A_{1,740}/(A_{1,740} + A_{1,630})$. Commercial pectins with determined DM were used as controls. Using this method, the DM of pectin from citrus (*Citrus*

spp.) fruit with 85% DM (Sigma) gave 75.1% ± 2.5% DM, pectin from citrus fruit with 55% to 70% DM (Sigma) gave 60.5% ± 1.5% DM, pectin from citrus fruit with 20% to 30% DM (Sigma) gave 26.9% ± 3.4% DM, and pectate sodium pectin from citrus fruit with DM of 8.6% (Sigma) gave 10.8% ± 0.9% DM. Three biological replicates for the wild type and the mutant were analyzed, and 10 acquisitions were acquired per biological sample.

Protein Extraction and Enzymatic Assay

Total proteins were extracted by grinding 2 mg of dry pollen grains in 50 mM sodium phosphate buffer, pH 7.5, 12.5 mM citric acid, 1 M NaCl, 0.2% (w/v) polyvinylpolypyrrolidone, and 0.01% (w/v) Tween 20 plus one tablet of protease inhibitor cocktail (Roche) for one night at 4°C. Cellular fragments were discarded by centrifugation at 10,000*g* for 45 min. The crude protein extract was concentrated by ultrafiltration on Amicon PM10 membranes (Millipore) in 50 mM sodium phosphate buffer, pH 7.5. Proteins were quantified by the micromethod of Bradford (1976), with the Bio-Rad kit and bovine serum albumin as a standard. PME activity was measured using the alcohol oxidase method according to Klavons and Bennett (1986). One international unit of PME activity induces the production of 1 μmol of methanol per min.

IEF and Zymography

IEF and zymography were performed as described by Paynel et al. (2014). Briefly, IEF of native proteins was performed on ultrathin polyacrylamide gels with a 6 to 10.5 pH range (Pharmalytes) in 5% acrylamide according to the manufacturer's procedure with the Multiphor II system (LKB Pharmacia). The pH gradient was measured with a contact electrode (pH Inlab 426; VWR International) along a central gel strip. Samples (20 μL) were loaded at the anodic side. After IEF, gels were washed for 15 to 30 min in 20 mM Tris-HCl, pH 8.5, and 5 mM EDTA. Activity of PME was then monitored in gel (zymogram) by using a sandwich of 1% (w/v) citrus pectin with a DM of 85% (Sigma) and 1% (w/v) agar according to Bertheau et al. (1984). The gel was incubated for 1 h at 25°C, and the demethylated pectins resulting from PME activities were precipitated with 0.1 M malic acid and stained with 0.02% (w/v) Ruthenium Red.

Statistical Analysis

Data were statistically treated using the GraphPad software (www.graphpad.com).

Supplemental Data

The following supplemental materials are available.

Supplemental Figure S1. Genomic organization of the *PME48* gene, location of the T-DNA, *PME48* expression in the mutant, and transcript sequence of *PME48*.

Supplemental Figure S2. Viability and phenotypic characteristics of wild-type and mutant lines.

Supplemental Figure S3. Germination rates of wild-type and *pme48−/−* pollen grains in liquid medium.

Supplemental Figure S4. Estimation of the growth speed in liquid medium of wild-type and *pme48−/−* pollen tubes.

Supplemental Table S1. List of primer pairs used for the qRT-PCR analyses.

Supplemental Movie S1. Time-lapse imaging of germination and tube growth of wild-type pollen grains.

Supplemental Movie S2. Time-lapse imaging of germination and tube growth of *pme48−/−* pollen grains.

ACKNOWLEDGMENTS

We thank the Research Network Végétal, Agronomie, Sol, et Innovation, PRIMACEN (Regional Platform for Cell Imaging), part of the Institute for Research and Innovation in Biomedicine of the Region Haute-Normandie, and the Fonds Européen de Développement Régional for the use of equipment. We also thank Dr. Claudine Morvan (Polymères, Biopolymères Surfaces, University of Rouen) for help on FT-IR analyses; Gaëlle Lucas and Carole Plasson (Glycobiologie et Matrice Extracellulaire Végétale, University of Rouen) for technical contributions in molecular biology and plant culture; and Dr. Bert De Rybel and Dolf Weijers (Laboratory of Biochemistry, Wageningen University) for the gift of the pPLV06 plasmid.

Received September 22, 2014; accepted December 16, 2014; published December 18, 2014.

LITERATURE CITED

Abràmoff MD, Magalhães PJ, Ram SJ (2004) Image processing with ImageJ. Biophotonics Int **11:** 36–42

Aouali N, Laporte P, Clément C (2001) Pectin secretion and distribution in the anther during pollen development in *Lilium*. Planta **213:** 71–79

Baskin TI, Busby CH, Fowke LC, Sammut M, Gubler F (1992) Improvements in immunostaining samples embedded in methacrylate: localization of microtubules and other antigens throughout developing organs in plants of diverse taxa. Planta **187:** 405–413

Bertheau Y, Madgidi-Hervan E, Kotoujansky A, Nguyen-The C, Andro T, Coleno A (1984) Detection of depolymerase isoenzymes after electrophoresis or electrofocusing, or in titration curves. Anal Biochem **139:** 383–389

Bethke G, Grundman RE, Sreekanta S, Truman W, Katagiri F, Glazebrook J (2014) Arabidopsis PECTIN METHYLESTERASEs contribute to immunity against *Pseudomonas syringae*. Plant Physiol **164:** 1093–1107

Boavida LC, McCormick S (2007) Temperature as a determinant factor for increased and reproducible *in vitro* pollen germination in *Arabidopsis thaliana*. Plant J **52:** 570–582

Bosch M, Cheung AY, Hepler PK (2005) Pectin methylesterase, a regulator of pollen tube growth. Plant Physiol **138:** 1334–1346

Bosch M, Hepler PK (2005) Pectin methylesterases and pectin dynamics in pollen tubes. Plant Cell **17:** 3219–3226

Bouton S, Leboeuf E, Mouille G, Leydecker MT, Talbotec J, Granier F, Lahaye M, Höfte H, Truong HN (2002) *QUASIMODO1* encodes a putative membrane-bound glycosyltransferase required for normal pectin synthesis and cell adhesion in *Arabidopsis*. Plant Cell **14:** 2577–2590

Bove J, Vaillancourt B, Kroeger J, Hepler PK, Wiseman PW, Geitmann A (2008) Magnitude and direction of vesicle dynamics in growing pollen tubes using spatiotemporal image correlation spectroscopy and fluorescence recovery after photobleaching. Plant Physiol **147:** 1646–1658

Bradford MM (1976) A rapid and sensitive method for the quantitation of microgram quantities of protein utilizing the principle of protein-dye binding. Anal Biochem **72:** 248–254

Brewbaker JL, Kwack BH (1963) The essential role of calcium ion in pollen germination and pollen tube growth. Am J Bot **50:** 859–865

Brummell DA, Harpster MH (2001) Cell wall metabolism in fruit softening and quality and its manipulation in transgenic plants. Plant Mol Biol **47:** 311–340

Caffall KH, Mohnen D (2009) The structure, function, and biosynthesis of plant cell wall pectic polysaccharides. Carbohydr Res **344:** 1879–1900

Castells T, Seoane-Camba JA, Suárez-Cervera M (2003) Intine wall modifications during germination of *Zygophyllum fabago* (Zygophyllaceae) pollen grains. Can J Bot **81:** 1267–1277

Catoire L, Pierron M, Morvan C, du Penhoat CH, Goldberg R (1998) Investigation of the action patterns of pectinmethylesterase isoforms through kinetic analyses and NMR spectroscopy: implications in cell wall expansion. J Biol Chem **273:** 33150–33156

Chebli Y, Geitmann A (2007) Mechanical principles governing pollen tube growth. Funct Plant Sci Biotech **1:** 232–245

Chebli Y, Kaneda M, Zerzour R, Geitmann A (2012) The cell wall of the Arabidopsis pollen tube: spatial distribution, recycling, and network formation of polysaccharides. Plant Physiol **160:** 1940–1955

Dai S, Li L, Chen T, Chong K, Xue Y, Wang T (2006) Proteomic analyses of *Oryza sativa* mature pollen reveal novel proteins associated with pollen germination and tube growth. Proteomics **6:** 2504–2529

Dardelle F, Lehner A, Ramdani Y, Bardor M, Lerouge P, Driouich A, Mollet JC (2010) Biochemical and immunocytological characterizations of Arabidopsis pollen tube cell wall. Plant Physiol **153:** 1563–1576

Dearnaley JD, Daggard GA (2001) Expression of a polygalacturonase enzyme in germinating pollen of *Brassica napus*. Sex Plant Reprod **13:** 265–271

Denès JM, Baron A, Renard CM, Péan C, Drilleau JF (2000) Different action patterns for apple pectin methylesterase at pH 7.0 and 4.5. Carbohydr Res **327:** 385–393

Derksen J, Knuiman B, Hoedemaekers K, Guyon A, Bonhomme S, Pierson ES (2002) Growth and cellular organization of *Arabidopsis* pollen tubes *in vitro*. Sex Plant Reprod **15:** 133–139

De Rybel B, van den Berg W, Lokerse A, Liao CY, van Mourik H, Möller B, Peris CL, Weijers D (2011) A versatile set of ligation-independent cloning vectors for functional studies in plants. Plant Physiol **156:** 1292–1299

Dumont M, Lehner A, Bouton S, Kiefer-Meyer MC, Voxeur A, Pelloux J, Lerouge P, Mollet JC (2014) The cell wall pectic polymer rhamnogalacturonan-II is required for proper pollen tube elongation: implications of a putative sialyltransferase-like protein. Ann Bot (Lond) **114:** 1177–1188

Durand C, Vicré-Gibouin M, Follet-Gueye ML, Duponchel L, Moreau M, Lerouge P, Driouich A (2009) The organization pattern of root border-like cells of Arabidopsis is dependent on cell wall homogalacturonan. Plant Physiol **150:** 1411–1421

Fayant P, Girlanda O, Chebli Y, Aubin CE, Villemure I, Geitmann A (2010) Finite element model of polar growth in pollen tubes. Plant Cell **22:** 2579–2593

Ferguson C, Teeri TT, Siika-Aho M, Read SM, Bacic A (1998) Location of cellulose and callose in pollen tubes and grains of *Nicotiana tabacum*. Planta **206:** 452–460

Francis KE, Lam SY, Copenhaver GP (2006) Separation of Arabidopsis pollen tetrads is regulated by *QUARTET1*, a pectin methylesterase gene. Plant Physiol **142:** 1004–1013

Fry SC (2011) Cell wall polysaccharide composition and covalent cross-linking. Annu Plant Rev **41:** 1–42

Ge LL, Tian HQ, Russell SD (2007) Calcium function and distribution during fertilization in angiosperms. Am J Bot **94:** 1046–1060

Ge LL, Xie CT, Tian HQ, Russell SD (2009) Distribution of calcium in the stigma and style of tobacco during pollen germination and tube elongation. Sex Plant Reprod **22:** 87–96

Ge W, Song Y, Zhang C, Zhang Y, Burlingame AL, Guo Y (2011) Proteomic analyses of apoplastic proteins from germinating *Arabidopsis thaliana* pollen. Biochim Biophys Acta **1814:** 1964–1973

Geitmann A, Steer M (2006) The architecture and properties of the pollen tube cell wall. In **R Malho**, ed, The Pollen Tube: Plant Cell Monographs, **Vol 3**. Springer-Verlag, Berlin, pp 177–200

Gnanasambandam R, Proctor A (2000) Determination of pectin degree of esterification by diffuse reflectance Fourier transform infrared spectroscopy. Food Chem **68:** 327–332

González-Carranza ZH, Elliott KA, Roberts JA (2007) Expression of polygalacturonases and evidence to support their role during cell separation processes in *Arabidopsis thaliana*. J Exp Bot **58:** 3719–3730

Gribaa A, Dardelle F, Lehner A, Rihouey C, Burel C, Ferchichi A, Driouich A, Mollet JC (2013) Effect of water deficit on the cell wall of the date palm (Phoenix dactylifera 'Deglet nour', Arecales) fruit during development. Plant Cell Environ **36:** 1056–1070

Guan Y, Guo J, Li H, Yang Z (2013) Signaling in pollen tube growth: crosstalk, feedback, and missing links. Mol Plant **6:** 1053–1064

Guénin S, Mareck A, Rayon C, Lamour R, Assoumou Ndong Y, Domon JM, Sénéchal F, Fournet F, Jamet E, Canut H, et al (2011) Identification of pectin methylesterase 3 as a basic pectin methylesterase isoform involved in adventitious rooting in *Arabidopsis thaliana*. New Phytol **192:** 114–126

Gutierrez L, Bussell JD, Păcurar DI, Schwambach J, Păcurar M, Bellini C (2009) Phenotypic plasticity of adventitious rooting in *Arabidopsis* is controlled by complex regulation of AUXIN RESPONSE FACTOR transcripts and microRNA abundance. Plant Cell **21:** 3119–3132

Harholt J, Suttangkakul A, Vibe Scheller H (2010) Biosynthesis of pectin. Plant Physiol **153:** 384–395

Hellens RP, Edwards EA, Leyland NR, Bean S, Mullineaux PM (2000) pGreen: a versatile and flexible binary Ti vector for Agrobacterium-mediated plant transformation. Plant Mol Biol **42:** 819–832

Hepler PK, Kunkel JG, Rounds CM, Winship LJ (2012) Calcium entry into pollen tubes. Trends Plant Sci **17:** 32–38

Holmes-Davis R, Tanaka CK, Vensel WH, Hurkman WJ, McCormick S (2005) Proteome mapping of mature pollen of *Arabidopsis thaliana*. Proteomics **5:** 4864–4884

Hruz T, Laule O, Szabo G, Wessendorp F, Bleuler S, Oertle L, Widmayer P, Gruissem W, Zimmermann P (2008) Genevestigator v3: a reference expression database for the meta-analysis of transcriptomes. Adv Bioinformatics **2008:** 420747

Huang L, Cao J, Zhang A, Ye Y, Zhang Y, Liu T (2009) The polygalacturonase gene *BcMF2* from *Brassica campestris* is associated with intine development. J Exp Bot **60:** 301–313

Iwano M, Shiba H, Miwa T, Che FS, Takayama S, Nagai T, Miyawaki A, Isogai A (2004) Ca^{2+} dynamics in a pollen grain and papilla cell during pollination of Arabidopsis. Plant Physiol **136:** 3562–3571

Jauh GY, Lord EM (1996) Localization of pectins and arabinogalactan-proteins in lily (*Lilium longiflorum* L.) pollen tube and style, and their possible roles in pollination. Planta **199:** 251–261

Jiang L, Yang SL, Xie LF, Puah CS, Zhang XQ, Yang WC, Sundaresan V, Ye D (2005) *VANGUARD1* encodes a pectin methylesterase that enhances pollen tube growth in the *Arabidopsis* style and transmitting tract. Plant Cell **17:** 584–596

Johnson MA, Lord EM (2006) Extracellular guidance cues and intracellular signaling pathways that direct pollen tube growth. In **R Malho**, ed, The Pollen Tube: A Cellular and Molecular Perspective, **Vol 3**. Springer, Heidelberg, pp 223–242

Johnson-Brousseau SA, McCormick S (2004) A compendium of methods useful for characterizing Arabidopsis pollen mutants and gametophytically-expressed genes. Plant J **39:** 761–775

Jolie RP, Duvetter T, Van Loey AM, Hendrickx ME (2010) Pectin methylesterase and its proteinaceous inhibitor: a review. Carbohydr Res **345:** 2583–2595

Kim J, Shiu SH, Thoma S, Li WH, Patterson SE (2006) Patterns of expansion and expression divergence in the plant polygalacturonase gene family. Genome Biol **7:** R87

Klavons JA, Bennett AD (1986) Determination of methanol using alcohol oxidase and its application to methyl ester content of pectins. J Agric Food Chem **34:** 597–599

Kremers GJ, Goedhart J, van Munster EB, Gadella TW Jr (2006) Cyan and yellow super fluorescent proteins with improved brightness, protein folding, and FRET Förster radius. Biochemistry **45:** 6570–6580

Lennon KA, Lord EM (2000) In vivo pollen tube cell of *Arabidopsis thaliana*. I. Tube cell cytoplasm and wall. Protoplasma **214:** 45–56

Li YQ, Chen F, Linskens HF, Cresti M (1994) Distribution of unesterified and esterified pectins in cell walls of pollen tubes of flowering plants. Sex Plant Reprod **7:** 145–152

Li YQ, Faleri C, Geitmann A, Zhang HQ, Cresti M (1995) Immunogold localization of arabinogalactan proteins, unesterified and esterified pectins in pollen grains and pollen tubes of *Nicotiana tabacum* L. Protoplasma **189:** 26–36

Louvet R, Cavel E, Gutierrez L, Guénin S, Roger D, Gillet F, Guerineau F, Pelloux J (2006) Comprehensive expression profiling of the pectin methylesterase gene family during silique development in *Arabidopsis thaliana*. Planta **224:** 782–791

Macquet A, Ralet MC, Loudet O, Kronenberger J, Mouille G, Marion-Poll A, North HM (2007) A naturally occurring mutation in an *Arabidopsis* accession affects a β-D-galactosidase that increases the hydrophilic potential of rhamnogalacturonan I in seed mucilage. Plant Cell **19:** 3990–4006

Manrique GD, Lajolo FM (2002) FT-IR spectroscopy as a tool for measuring degree of methyl esterification in pectins isolated from ripening papaya fruit. Postharvest Biol Technol **25:** 99–107

Micheli F (2001) Pectin methylesterases: cell wall enzymes with important roles in plant physiology. Trends Plant Sci **6:** 414–419

Mollet JC, Leroux C, Dardelle F, Lehner A (2013) Cell wall composition, biosynthesis and remodeling during pollen tube growth. Plants **2:** 107–147

Mollet JC, Park SY, Nothnagel EA, Lord EM (2000) A lily stylar pectin is necessary for pollen tube adhesion to an in vitro stylar matrix. Plant Cell **12:** 1737–1750

Mouille G, Ralet MC, Cavelier C, Eland C, Effroy D, Hématy K, McCartney L, Truong HN, Gaudon V, Thibault JF, et al (2007) Homogalacturonan synthesis in *Arabidopsis thaliana* requires a Golgi-localized protein with a putative methyltransferase domain. Plant J **50:** 605–614

Nguema-Ona E, Coimbra S, Vicré-Gibouin M, Mollet JC, Driouich A (2012) Arabinogalactan proteins in root and pollen-tube cells: distribution and functional aspects. Ann Bot (Lond) **110:** 383–404

Palanivelu R, Tsukamoto T (2012) Pathfinding in angiosperm reproduction: pollen tube guidance by pistils ensures successful double fertilization. Wiley Interdiscip Rev Dev Biol **1:** 96–113

Palin R, Geitmann A (2012) The role of pectin in plant morphogenesis. Biosystems **109:** 397–402

Parre E, Geitmann A (2005a) Pectin and the role of the physical properties of the cell wall in pollen tube growth of *Solanum chacoense*. Planta **220:** 582–592

Parre E, Geitmann A (2005b) More than a leak sealant: the mechanical properties of callose in pollen tubes. Plant Physiol **137:** 274–286

Paynel F, Leroux C, Surcouf O, Schaumann A, Pelloux J, Driouich A, Mollet JC, Lerouge P, Lehner A, Mareck A (2014) Kiwi fruit PMEI inhibits PME activity, modulates root elongation and induces pollen tube burst in *Arabidopsis thaliana*. Plant Growth Regul **74:** 285–297

Peaucelle A, Braybrook SA, Le Guillou L, Bron E, Kuhlemeier C, Höfte H (2011) Pectin-induced changes in cell wall mechanics underlie organ initiation in *Arabidopsis*. Curr Biol **21:** 1720–1726

Peaucelle A, Louvet R, Johansen JN, Höfte H, Laufs P, Pelloux J, Mouille G (2008) Arabidopsis phyllotaxis is controlled by the methyl-esterification status of cell-wall pectins. Curr Biol **18:** 1943–1948

Phan TD, Bo W, West G, Lycett GW, Tucker GA (2007) Silencing of the major salt-dependent isoform of pectinesterase in tomato alters fruit softening. Plant Physiol **144:** 1960–1967

Qin Y, Chen D, Zhao J (2007) Localization of arabinogalactan proteins in anther, pollen, and pollen tube of *Nicotiana tabacum* L. Protoplasma **231:** 43–53

Qin Y, Leydon AR, Manziello A, Pandey R, Mount D, Denic S, Vasic B, Johnson MA, Palanivelu R (2009) Penetration of the stigma and style elicits a novel transcriptome in pollen tubes, pointing to genes critical for growth in a pistil. PLoS Genet **5:** e1000621

Rafińska K, Świdziński M, Bednarska-Kozakiewicz E (2014) Homogalacturonan deesterification during pollen-ovule interaction in *Larix decidua* Mill.: an immunocytochemical study. Planta **240:** 195–208

Rejón JD, Delalande F, Schaeffer-Reiss C, Carapito C, Zienkiewicz K, de Dios Alché J, Rodríguez-García MI, Van Dorsselaer A, Castro AJ (2013) Proteomics profiling reveals novel proteins and functions of the plant stigma exudate. J Exp Bot **64:** 5695–5705

Rhee SY, Somerville CR (1998) Tetrad pollen formation in *quartet* mutants of *Arabidopsis thaliana* is associated with persistence of pectic polysaccharides of the pollen mother cell wall. Plant J **15:** 79–88

Röckel N, Wolf S, Kost B, Rausch T, Greiner S (2008) Elaborate spatial patterning of cell-wall PME and PMEI at the pollen tube tip involves PMEI endocytosis, and reflects the distribution of esterified and de-esterified pectins. Plant J **53:** 133–143

Roy S, Eckard KJ, Lancelle S, Hepler PK, Lord EM (1997) High-pressure freezing improves the ultrastructural preservation of *in vivo* grown lily pollen tubes. Protoplasma **200:** 87–98

Sénéchal F, Wattier C, Rustérucci C, Pelloux J (2014) Homogalacturonan-modifying enzymes: structure, expression, and roles in plants. J Exp Bot **65:** 5125–5160

Suárez-Cervera M, Arcalis E, Le Thomas A, Seoane-Camba JA (2002) Pectin distribution pattern in the apertural intine of *Euphorbia peplus* L. (Euphorbiaceae) pollen. Sex Plant Reprod **14:** 291–298

Suárez-Cervera M, Asturias JA, Vega-Maray A, Castells T, López-Iglesias C, Ibarrola I, Arilla MC, Gabarayeva N, Seoane-Camba JA (2005) The role of allergenic proteins Pla a1 and Pla a2 in the germination of *Platanus acerifolia* pollen grains. Sex Plant Reprod **18:** 101–112

Tian GW, Chen MH, Zaltsman A, Citovsky V (2006) Pollen-specific pectin methylesterase involved in pollen tube growth. Dev Biol **294:** 83–91

Tieman DM, Handa AK (1994) Reduction in pectin methylesterase activity modifies tissue integrity and cation levels in ripening tomato (*Lycopersicon esculentum* Mill.) fruits. Plant Physiol **106:** 429–436

Van Aelst AC, Van Went JL (1992) Ultrastructural immuno-localization of pectins and glycoproteins in *Arabidopsis thaliana* pollen grains. Protoplasma **168:** 14–19

Vandesompele J, De Preter K, Pattyn F, Poppe B, Van Roy N, De Paepe A, Speleman F (2002) Accurate normalization of real-time quantitative RT-PCR data by geometric averaging of multiple internal control genes. Genome Biol **3:** research0034

Verhertbruggen Y, Marcus SE, Haeger A, Ordaz-Ortiz JJ, Knox JP (2009) An extended set of monoclonal antibodies to pectic homogalacturonan. Carbohydr Res **344:** 1858–1862

Vincken JP, Schols HA, Oomen RJ, McCann MC, Ulvskov P, Voragen AG, Visser RG (2003) If homogalacturonan were a side chain of rhamnogalacturonan I: implications for cell wall architecture. Plant Physiol **132:** 1781–1789

Vogler H, Draeger C, Weber A, Felekis D, Eichenberger C, Routier-Kierzkowska AL, Boisson-Dernier A, Ringli C, Nelson BJ, Smith RS, et al (2013) The pollen tube: a soft shell with a hard core. Plant J **73:** 617–627

Walker M, Tehseen M, Doblin MS, Pettolino FA, Wilson SM, Bacic A, Golz JF (2011) The transcriptional regulator LEUNIG_HOMOLOG regulates mucilage release from the Arabidopsis testa. Plant Physiol **156:** 46–60

Wang Y, Zhang WZ, Song LF, Zou JJ, Su Z, Wu WH (2008) Transcriptome analyses show changes in gene expression to accompany pollen germination and tube growth in Arabidopsis. Plant Physiol **148:** 1201–1211

Wen F, Zhu Y, Hawes MC (1999) Effect of pectin methylesterase gene expression on pea root development. Plant Cell **11:** 1129–1140

Western TL, Burn J, Tan WL, Skinner DJ, Martin-McCaffrey L, Moffatt BA, Haughn GW (2001) Isolation and characterization of mutants defective in seed coat mucilage secretory cell development in Arabidopsis. Plant Physiol **127:** 998–1011

Willats WGT, Orfila C, Limberg G, Buchholt HC, van Alebeek GJ, Voragen AG, Marcus SE, Christensen TM, Mikkelsen JD, Murray BS, et al (2001) Modulation of the degree and pattern of methyl-esterification of pectic homogalacturonan in plant cell walls: implications for pectin methyl esterase action, matrix properties, and cell adhesion. J Biol Chem **276:** 19404–19413

Winship LJ, Obermeyer G, Geitmann A, Hepler PK (2010) Under pressure, cell walls set the pace. Trends Plant Sci **15:** 363–369

Winter D, Vinegar B, Nahal H, Ammar R, Wilson GV, Provart NJ (2007) An "Electronic Fluorescent Pictograph" browser for exploring and analyzing large-scale biological data sets. PLoS ONE **2:** e718

Wolf S, Mouille G, Pelloux J (2009a) Homogalacturonan methyl-esterification and plant development. Mol Plant **2:** 851–860

Wolf S, Rausch T, Greiner S (2009b) The N-terminal pro region mediates retention of unprocessed type-I PME in the Golgi apparatus. Plant J **58:** 361–375

Zerzour R, Kroeger J, Geitmann A (2009) Polar growth in pollen tubes is associated with spatially confined dynamic changes in cell mechanical properties. Dev Biol **334:** 437–446

Zhang GF, Staehelin LA (1992) Functional compartmentation of the Golgi apparatus of plant cells: immunocytochemical analysis of high-pressure frozen- and freeze-substituted sycamore maple suspension culture cells. Plant Physiol **99:** 1070–1083

Zhang X, Henriques R, Lin SS, Niu QW, Chua NH (2006) Agrobacterium-mediated transformation of *Arabidopsis thaliana* using the floral dip method. Nat Protoc **1:** 641–646

Zhao J, Yang HY, Lord EM (2004) Calcium levels increase in the lily stylar transmitting tract after pollination. Sex Plant Reprod **16:** 259–263

Zhu Y, Zhao P, Wu X, Wang W, Scali M, Cresti M (2011) Proteomic identification of differentially expressed proteins in mature and germinated maize pollen. Acta Physiol Plant **33:** 1467–1474